Manifestations of Radiation Hormesis in Biological Fluids Exposed to Low-Flux Neutron Irradiation: Insights from IR Spectroscopy and Biochemical Analysis

Mahsud Barot Islomzoda , Khamidullo Khabibulloev , Matrobiyon Mehrob Khurramzod , Dilshod Nematov *

Posted Date: 31 March 2026

doi: 10.20944/preprints202603.2309.v1

Keywords: IR spectroscopy; blood serum; chicken egg serum; thermal neutrons; low flux; biochemical analysis; radiation hormesis; structural changes

 doi:10.20944/preprints202603.2309.v1

Article

Manifestations of Radiation Hormesis in Biological Fluids Exposed to Low-Flux Neutron Irradiation: Insights from IR Spectroscopy and Biochemical Analysis

Mahsud Barot Islomzoda [1], Khamidullo Khabibulloev [2], Matrobiyon Mehrob Khurramzod [1] and Dilshod Nematov [3,4,*]

[1] Tajik National University, Dushanbe 734025, Tajikistan
[2] Khujand Scientific Center of the National Academy of Sciences of Tajikistan, Khujand 735700, Tajikistan
[3] S. Umarov Physical-Technical Institute of NAST, Dushanbe 734063, Tajikistan
[4] School of Optoelectronic Engineering and CQUPT Innovation Institute - BUL , Chongqing University of Posts and Telecommunications, Chongqing 400065, China
* Correspondence: dilnem@mail.ru

Abstract

This study presents a comprehensive comparative assessment of the structural and functional responses of human serum and hen egg serum to natural aging (3, 5, and 7 days) and low thermal neutron fluxes (1.3×10^8, 2.16×10^8, and 3×10^8 N/cm^2). Structural changes were investigated using Fourier transform infrared spectroscopy (FTIR), and biochemical parameters were used to assess functional changes. Natural aging induced progressive negative frequency shifts in the region of 1080-1340 cm^{-1} consistent with dehydration, increased hydrogen bonding, and decreased mobility of lipid and protein components. In contrast, neutron irradiation produced predominantly positive frequency shifts (+3 to +8 cm^{-1}), with the most pronounced effects observed at an intermediate flux density of 2.16×10^8 N/cm^2. These changes indicate a weakening of hydrogen bonds, a redistribution of electron density within amide and phosphate groups, and a partial reorganization of the protein-lipid matrix. Biochemical analysis correlates with spectroscopic observations: natural aging was associated with a decrease in total protein content and a moderate increase in ALT and AST activities, whereas neutron irradiation stimulated enzymatic activity and metabolic parameters in a nonlinear, flux-dependent manner. It is assumed that the observed non-monotonic reaction with a maximum effect at an intermediate neutron flux is caused by low-flux hormesis of thermal neutrons. Overall, the results show that low-flux neutron irradiation induces adaptive structural and functional responses in biological fluids that are fundamentally different from passive aging processes, highlighting the potential of IR spectroscopy as a sensitive tool for detecting molecular-level changes induced by low-flux neutron exposure. The observed non-monotonic responses are consistent with a hormetic-like interpretation, though further studies are needed to confirm this mechanism.

Keywords: IR spectroscopy; blood serum; chicken egg serum; thermal neutrons; low flux; biochemical analysis; radiation hormesis; structural changes

1. Introduction

The biological effects of low-dose, low-flux ionizing radiation have attracted considerable attention in recent decades, as numerous studies demonstrate that living systems can exhibit nonlinear, adaptive, or even stimulatory responses at radiation levels significantly lower than those associated with damage [1–4]. This concept, widely known as radiation hormesis, posits that low-

 doi:10.20944/preprints202603.2309.v1

dose, low-flux irradiation can activate protective molecular pathways, alter protein-lipid interactions, and promote compensatory metabolic shifts rather than induce destructive changes [5–7]. Such adaptive behavior has been documented for various types of ionizing radiation, including thermal neutrons, whose interactions with biomolecules occur primarily through secondary charged particles and localized ionization events [8].

Thermal neutrons represent a particularly interesting case for biophysical studies, as their low-energy interactions can disrupt hydration shells, electron density distributions, and hydrogen bond networks without causing extensive radiolysis. Several studies have shown that low-flux thermal neutrons can induce measurable structural changes in whole blood and serum biomolecules, detectable by infrared spectroscopy and biochemical assays [9–14]. These studies suggest the existence of dose-dependent, non-monotonic responses, where intermediate neutron fluxes can cause the strongest structural modulation, consistent with hormetic response patterns [5,7].

Fourier transform infrared (FTIR) spectroscopy is a powerful tool for monitoring changes in molecular structure and microenvironment in complex biological matrices. Even minor shifts in the vibrational frequencies of amide, lipid, and phosphate groups can serve as markers of protein conformational rearrangements, lipid ordering, hydration state, and intermolecular interactions [15–18]. FTIR analysis is widely used to detect structural abnormalities in serum, including disease-specific changes, dehydration effects, and radiation-induced modifications [10,17,19–23]. Its sensitivity to hydrogen bond strength and side-chain mobility makes FTIR particularly suitable for distinguishing natural degradation processes from adaptive radiation-induced restructuring.

Natural aging of biological fluids such as human serum and egg serum involves dehydration, oxidation, and gradual stabilization of protein-lipid complexes, which typically manifests as negative spectral shifts and narrowing of bands in the 1080-1340 cm^{-1} and 2800-3000 cm^{-1} [12,17,22]. In contrast, low-flux neutron exposure has been reported to induce positive spectral shifts, broadening of key bands, or partial relaxation effects reflecting weakening of hydrogen bonds, changes in the electron environment, and reorganization of tertiary structural elements [9–14]. Thus, direct comparison of neutron-induced aging and changes represents a valuable strategy for identifying radiation-specific spectral markers. Complementary computational and experimental approaches have also contributed to understanding radiation-induced molecular rearrangements in complex biosystems and related materials [24–29].

The aim of this study is to conduct a comprehensive comparative analysis of the effects of natural aging (3, 5, 7 days) and low-flux thermal neutron irradiation (1.3×10^8, 2.16×10^8 and 3×10^8 Neutron-induced changes (neutrons/cm^2) in human serum and chicken egg serum are studied. Using Fourier transform infrared (FTIR) spectroscopy and biochemical analysis (ALT, AST, total protein, glucose), we investigate structure-function correlations and assess whether neutron-induced changes follow nonlinear adaptive patterns distinct from passive degradation. By integrating spectral and biochemical data, this work aims to identify diagnostic markers for low-dose neutron exposure and contribute to a biophysical understanding of the mechanism of hormesis in response to other factors. This study is exploratory in nature and focuses on molecular-level structural responses using samples from a single human donor, with the understanding that biological variability will be addressed in subsequent investigations.

2. Materials and Methods

Human serum was obtained by centrifugation of whole blood collected from a healthy volunteer. The donor provided written informed consent. The study was conducted in accordance with the ethical standards of the institutional review board of Tajik National University (Approval No. IRB-2023-017). Chicken egg serum was isolated from fresh eggs of a local breed. Both types of serum were used as model liquid biosystems with similar protein-lipid compositions but different structural stability and water-binding capacity. Immediately after preparation, samples were placed in sterile plastic containers and divided into control and experimental series. Control samples were stored at room temperature (22 ± 2 °C) for 3, 5, and 7 days. Experimental samples were exposed to low thermal

 doi:10.20944/preprints202603.2309.v1

neutron fluxes with fluences of 1.3×10^8 and 2.16×10^8 and 3×10^8 N/cm^2 through equal time intervals. Before IR spectroscopic analysis, all serum samples were dried at 60 °C to a paste-like state to eliminate the influence of water on the IR spectra. The conditions for preparing samples for recording IR spectra have the following effects: when drying at 60 °C, for over three hours, water is practically removed from the whey samples, proteins are partially denatured, and their structure changes. This is a partial limitation of the method. However, it can be assumed that, since all samples are subjected to identical conditions, the changes during preparation for spectral recording are identical for all samples. The observed differences are the result of the effects of natural aging and thermal neutron irradiation on the whey samples we studied before drying and appear after exposure to the experimental conditions. The dried samples were ground and mixed with spectroscopic KBr, then pressed into tablets under pressure. A specially designed setup with a radioisotope neutron source was used to irradiate the test samples. The setup's main component was a cubic protective tank made of 4 mm thick sheet iron. The tank's geometric dimensions were 70x70x70 cm. The tank's interior was primarily filled with paraffin, which acted as a neutron moderator and reduced their energy to thermal values. A cylindrical channel was formed in the tank's central section, housing a plutonium-beryllium neutron source. This channel was 25 cm high and 3.7 cm in diameter. This channel served as a fast neutron channel, since a high-energy neutron flux is generated in the immediate vicinity of the source. The fast neutron channel was surrounded by a 5 cm thick paraffin layer, which served as a moderator. Behind this layer was a second channel, a thermal neutron channel 2.6 cm wide. This design ensured gradual moderation of fast neutrons in the paraffin and the formation of a stable thermal neutron flux in the outer channel, where the test samples were irradiated. In this study, a plutonium-beryllium (Pu-Be) radioisotope source, belonging to the (α,n) type, was used as a neutron source. Of all the known plutonium isotopes, only three are practically used to create neutron sources: ^{238}Pu, ^{239}Pu, and ^{240}Pu. In this study, a fast neutron source based on the isotope ^{239}Pu was fabricated. The neutron source was made of an intermetallic compound of plutonium and beryllium, $PuBe_{13}$. Crystals of the $PuBe_{13}$ compound with geometric dimensions of about 2-10 μm are distributed in a beryllium matrix. The thermal neutron flux was determined using standard methods based on neutron activation. To ensure radiation safety, the source was placed within a cadmium layer, which served as additional shielding from neutron radiation [5,10,12–14,20].

FTIR spectra were recorded on an IR Affinity-1S spectrometer (Shimadzu, Japan) in the spectral range from 4000 to 400 cm^{-1}. With a spectral resolution of 0.5 cm^{-1}. Each spectrum was scanned at least three times. Reproducibility was ±0.25 cm $^{-1}$ The objective was to study the frequency shift at the absorption band maxima. To ensure the accuracy of the observed shifts, single, non-overlapping absorption bands were used. Because the primary objective was to assess the direction and magnitude of frequency shifts rather than to compare group means, inferential statistical testing was not applied. All reported shifts are based on the mean values from five replicate measurements, and the focus is on the reproducibility of peak positions rather than on hypothesis testing. Changes in absorption band intensity were not part of the study. Therefore, normalization, deconvoluted, and approximated measurements were not performed, and there was no need to select the correct baseline or perform multivariate analysis. The following spectral regions were analyzed: 1080-1240 cm^{-1} for phosphate vibrations, 1310-1460 cm^{-1} for deformation vibrations of CH_2 and CH_3, 2800-3000 cm^{-1} for stretching vibrations of aliphatic CH and 3060-3080 cm^{-1} for vibrations of aromatic CH. For each sample, peak positions, frequency shifts relative to the control, and changes in band intensity and width were assessed. Biochemical parameters were measured to correlate functional and structural changes. Alanine aminotransferase (ALT) and aspartate aminotransferase (AST) activities were determined in U/L, total protein in g/L , and glucose in mmol/L. All measurements were performed in triplicate and presented as mean values. All experimental measurements were performed in 5 replicates to ensure the reliability of the data obtained. The presented results are the mean values obtained on the basis of 5 independent measurements.It should be noted that human serum was obtained from a single healthy donor. This limits the generalizability of the findings with

 doi:10.20944/preprints202603.2309.v1

respect to interindividual biological variability, and the results should be interpreted as a demonstration of molecular-level structural responses rather than population-level trends.

3. Results and Discussion

Figure 1 shows the infrared spectrum of human blood serum exposed to air for three days. It demonstrates the key vibrational characteristics associated with the protein-lipid matrix of the sample and illustrates the characteristic changes in the sample's spectral profile.

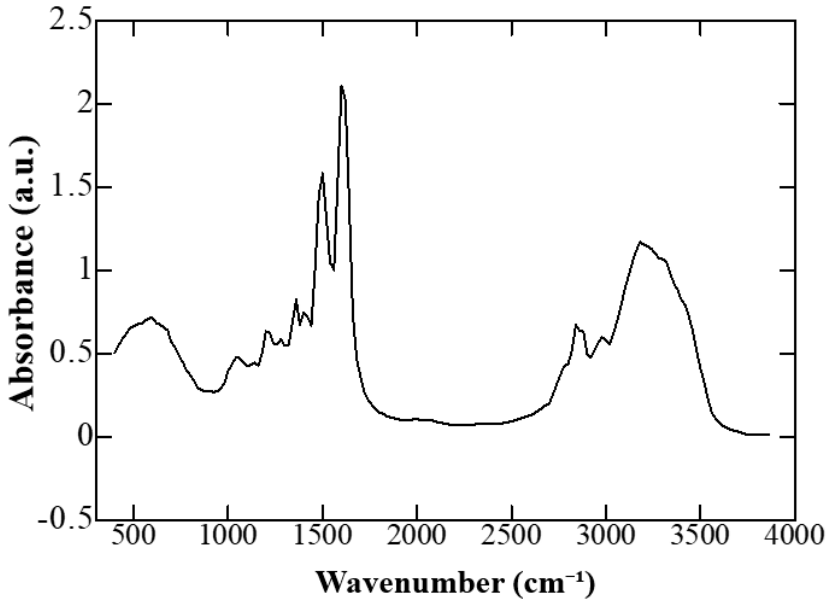

Figure 1. IR spectrum of human blood serum after exposure to air for 3 days.

The spectrum is characterized by prominent absorption bands in regions corresponding to amide I and amide II vibrations, indicating the presence of whey proteins, as well as bands associated with stretching and bending vibrations of lipid-associated C-H bonds. Changes in band intensity and shape reflect molecular rearrangements occurring during air exposure, associated with partial dehydration and conformational modifications of biomolecular components. Table 1 presents the main absorption bands and their assignment to the corresponding functional groups, reflecting the structural features of the protein-lipid complex.

Table 1. Frequencies of absorption bands of the most important characteristic groups in the blood serum of healthy people.

Wavenumber (cm^{-1})	Purpose	Functional Groups / Compounds
3207 (3192)	↔ Stretching	Linked -OH and -NH groups
3020-3000	↔ Stretching	=CH; unsaturated fatty acids; cholesterol esters
2990-2950	$\leftrightarrow_{as}$ Stretching	$-CH_3$; cholesterol esters; triglycerides
2950-2880	$\leftrightarrow_{as}$ Stretching	$-CH_2$; fatty acids; phospholipids

 doi:10.20944/preprints202603.2309.v1

2880-2860	$\leftrightarrow_{as}$ Stretching	-CH_3; cholesterol esters; triglycerides; glycerol
2870-2830	$\leftrightarrow_{s}$ Stretching	-C H_2; fatty acids; phospholipids
1480-1430	$\Leftarrow_{as}$ / $\Leftarrow_{s}$ Bend	-CH_3, -CH_2; fatty acids; phospholipids; triglycerides
1430-1360	$\leftrightarrow$ Stretching	-COO^-; amino acids
1311 (1300)	$\Leftarrow$ Bending	-NH_3^+
1244 (1241)	$\leftrightarrow$ / $\leftrightarrow_{as}$ Stretching	-C-OH, acetate groups; -C-O-C-; asymmetric O-P=O
1084 (1076)	$\leftrightarrow_{s}$ Stretching	-C-P-O (PO_3^{2-}); -C-OH
Legend: $\leftrightarrow$ - tensile vibrations, $\Leftarrow$ - bending vibrations, $_s$ - symmetrical vibrations, $_{as}$ - asymmetric oscillations		

The spectral profile presented in Table 1 is consistent with previously described characteristics of IR spectra of healthy human serum, including the dominant contribution of protein amide bands, lipid methylene stretching vibrations, and phosphate-related absorptions, as described in earlier spectroscopic studies [15–18].

3.1. Comparison of Air-Exposed Blood Serum and Egg Serum Samples

FTIR spectra were recorded for blood serum and egg whey after 3, 5, and 7 days of incubation. Particular attention was paid to the bands corresponding to C=O, N-H, C-H, P=O, and C-O vibrations, which are sensitive to hydrogen bonds and the secondary structure of the protein [12]. During incubation of the samples for 3, 5, and 7 days, successive changes in the frequencies of characteristic absorption bands were observed, reflecting transformations in the hydrogen bond network and the structure of protein molecules. In human serum, a negative frequency shift was recorded in most spectral regions (Table 2). The band at 1080 cm^{-1} (stretching vibrations of PO_2) shifted up to 1075 cm^{-1}, 1242 cm^{-1} (asymmetric stretching vibrations of PO_2) shifts to 1235 cm^{-1}, and in the region of 1315-1342 cm^{-1} (deformation vibrations of CH_2 and CH_3) frequencies decrease by 4-6 cm^{-1}. Similar shifts are also observed in the lipid regions at 1454-1449 cm^{-1}, 2927-2923 cm^{-1} and 2958-2955 cm^{-1}. This trend in spectral changes indicates increased hydrogen bonding and dehydration of the protein-lipid matrix, as well as a partial decrease in the mobility of amino acid side chains. Shifts in the region of 1080-1240 cm^{-1} corresponding to phosphate groups, reflect the stabilization of electronic states and structural «maturation» of proteins during aging (Table 2). Aging of human blood serum resulted in systematic negative frequency shifts in the main vibrational regions, including the stretching vibrations of phosphate groups (1082→1080→1080 cm^{-1}), amine-related bending vibrations and CH_2/CH_3 deformation bands.

Table 2. Main frequencies of the absorption bands of the IR spectrum of blood serum samples from elderly people.

No.	3 days, no exposure	5 days, no aging	Difference between samples not aged for 3 and 5 days	7 days, no aging	Difference between samples not aged for 3 and 7 days
	ν_3, cm^{-1}	ν_5, cm^{-1}	ν_3-ν_5	ν_7, cm^{-1}	ν_3-ν_7

 doi:10.20944/preprints202603.2309.v1

1	1082	1080	2	1080	2
2	1242	1244	-2	1242	0
3	1315	1317	-2	1311	4
4	1342	1346	-4	1342	0
5	1398	1398	0	1400	-2
6	1454	1452	2	1452	2
7	2872	2872	0	2872	0
8	2927	2931	-4	2931	-4
9	2958	2958	0	2956	2
10	3068	3066	2	3068	0

These changes indicate progressive dehydration, increased hydrogen bonding, and decreased conformational mobility of protein side chains. The most pronounced changes were observed between days 3 and 7, indicating a gradual compaction of the protein-lipid matrix.

As shown in Table 3, similar changes in chicken egg serum are expressed much less sharply: the amplitude of the shifts does not exceed 2-5 cm^{-1}, while the bands in the range of 1313-1340 cm^{-1} retain virtually unchanged shape and intensity. Minor changes are observed in the range of 2872-2958 cm^{-1}, where minimal fluctuations in the frequency of methyl and methylene groups are recorded. These results indicate a higher structural stability of the protein-lipid complexes of ovalbumin, which provide the egg serum's buffering capacity and resistance to dehydration. Consequently, during the natural aging process, blood serum exhibits greater lability, whereas chicken egg serum exhibits relative structural inertia. [13,19,20].

Table 3. Main frequencies of the absorption bands of the IR spectrum of whey samples from aged chicken eggs.

No.	3 days, no exposure	5 days, no aging	Difference between samples not aged for 3 and 5 days.	7 days, no aging	Difference between samples not aged for 3 and 7 days.
	ν_3, cm^{-1}	ν_5, cm^{-1}	ν_3-ν_5	ν_7, cm^{-1}	ν_3-ν_7
1	1080	1074	6	1082	-2
2	1238	1238	0	1238	0
3	1311	1311	0	1311	0
4	1338	1338	0	1342	-4
5	1396	1396	0	1396	0
6	1454	1454	0	1454	0
7	2873	2875	-2	2875	-2
8	2937	2939	-2	2935	2
9	2962	2960	2	2958	4
10	3070	3068	2	3066	4

Compared to human serum, chicken egg serum exhibited significantly smaller spectral shifts during aging. Most vibrational frequencies remained unchanged or varied within ±2-4 cm^{-1}, indicating greater structural stability and greater buffering capacity of the ovalbumin-rich matrix.

 doi:10.20944/preprints202603.2309.v1

This supports the hypothesis that egg serum is less susceptible to aging-induced restructuring. dehydration.

3.2. Comparison of Irradiated Human Blood Serum and Chicken Egg Serum Samples

Exposure to low thermal neutron fluxes leads to more complex changes in spectral characteristics. Unlike natural aging, both negative and positive shifts are observed, indicating structural adaptation and reorganization of intramolecular bonds. As can be seen from Table 4, exposure to low thermal neutron fluxes (1.3×10^8 - 3×10^8 N/cm^2) causes opposite changes: positive frequency shifts are observed in all key spectral regions, on average from +3 to +8 cm^{-1}. In human blood serum, the band at 1080 cm^{-1} shifts to 1084 cm^{-1}, from 1242 cm^{-1} to 1249 cm^{-1}, from 1315 cm^{-1} to 1322 cm^{-1}, and from cm^{-1} to 1350 cm^{-1}. In the lipid regions, frequencies increase from 2927 to 2933 cm^{-1} and from 2958 to 2962 cm^{-1}, while in the 3068-3072 cm^{-1} region, an increase in the vibration frequency of aromatic =C-H bonds is observed. This pattern of spectral shifts indicates a weakening of intermolecular hydrogen bonds, a redistribution of electron density in the phosphate and amide groups, and a partial reorganization of the tertiary structure of the protein. The most pronounced changes are observed in the ranges of 1310-1340 and 2920-2960 cm^{-1} ranges reflecting the dynamics of lipid components and changes in the microenvironment of protein-lipid interfaces.

Table 4. Main frequencies of the absorption bands of the IR spectrum of irradiated human blood serum samples.

No.	1.3×10^8 N/cm^2	2.16×10^8 N/cm^2	The difference between 3 and 5 days	3×10^8 N/cm^2	Difference between samples not aged for 3 and 7 days.
	ν_3, cm^{-1}	ν_5, cm^{-1}	ν_3-ν_5	ν_7, cm^{-1}	ν_3-ν_7
1	1078	1080	-2	1082	-4
2	1240	1238	2	1240	0
3	1313	1315	-2	1311	2
4	1340	1346	-6	1342	-2
5	1398	1398	0	1398	0
6	1454	1454	0	1454	0
7	2873	2873	0	2873	0
8	2931	2929	-2	2931	0
9	2956	2962	-6	2960	-4
10	3066	3066	0	3066	0

Exposure to low thermal neutron fluxes resulted predominantly in positive frequency shifts in the infrared ranges of human blood serum, particularly at an intermediate flux of 2.16×10^8 N/cm^2. Neutron interactions with the sample matrix can generate secondary charged particles and localized ionization events, which may perturb hydration shells and alter the hydrogen bonding network. Such perturbations are consistent with the observed positive frequency shifts and the reorganization of protein-lipid interfaces. This pattern suggests a partial weakening of hydrogen bonds and a redistribution of electron density within amide and phosphate groups. Notably, a nonlinear response is observed. Maximum frequency shift at the intermediate dose followed by partial relaxation at the highest dose. It is assumed that This is consistent with the concept of adaptive (hormetic) restructuring rather than cumulative degradation.

 doi:10.20944/preprints202603.2309.v1

Of particular interest is the nonlinear nature of the dose-effect relationship: at an average flow (2.16×10^8 N/cm^2) shifts reach their maximum, whereas at a higher flux (3×10^8 N/cm^2), the frequencies partially return to their original values. This effect reveals part of the possible mechanism of the adaptive response of a biosystem to an average flux, in which moderate fluxes activate structural and functional rearrangements, while higher fluxes trigger compensatory stabilization mechanisms. This behavior is analogous to the concept of radiation hormesis [5,10,12,20], according to which low doses of ionizing radiation cause regulatory and stimulating effects rather than damage.

The IR spectra of chicken egg serum are compared under the influence of thermal neutrons at doses of 1.3×10^8, 2.16×10^8 and 3×10^8 N/cm^2. (Table 5) Similar, but less pronounced, trends are observed. The absorption band frequencies shift by an average of +3…+5 cm^{-1} (1080 → 1083, 1242 → 1247, 1313 → 1318, 1340 → 1345 cm^{-1}) , with the changes being gradual and partially reversible, indicating a higher stability of the protein-lipid structure of ovalbumin. Unlike blood serum, no significant broadening of the bands is observed, indicating a lesser degree of hydrogen bond destabilization and greater self-stabilizing capacity of egg serum. Thus, chicken egg serum exhibits a milder and more balanced response to low-flux neutron irradiation, confirming its reliability as a model protein system.

Table 5. Main frequencies of absorption bands in the IR spectra of irradiated samples of chicken egg serum.

No.	1.3×10^8 N/cm^2	2.16×10^8 N/cm^2	The difference between 3 and 5 days	3×10^8 N / cm^2	The difference between 3 and 7-day
	ν_3, cm^{-1}	ν_5, cm^{-1}	ν_3-ν_5	ν_7, cm^{-1}	ν_3-ν_7
1	1078	1076	2	1080	-2
2	1238	1238	0	1240	-2
3	1313	1311	2	1311	0
4	1340	1342	-2	1344	-4
5	1396	1396	0	1398	-2
6	1454	1452	2	1454	0
7	2875	2875	0	2873	-2
8	2935	2935	0	2937	-2
9	2962	2962	0	2962	0
10	3066	3070	-4	3066	0

The spectral responses of chicken egg serum to neutron irradiation were generally weaker than those of human serum. Moderate positive shifts were detected, but their overall magnitude remained limited, supporting the interpretation that the ovalbumin-based system exhibits intrinsic stability both against structural dehydration and against thermal neutron flux-induced perturbations.

3.3. Biochemical Analysis and Comparison with IR Spectroscopy Data

To determine whether the structural changes detected by IR spectroscopy were accompanied by functional biochemical changes, a biochemical analysis of blood serum was performed. Alanine aminotransferase and aspartate aminotransferase activities , as well as total protein and glucose concentrations, were selected as sensitive indicators of enzymatic activity, protein integrity, and metabolic status. These parameters are known to respond to both degradative and adaptive biochemical processes. The quantitative results obtained for naturally aged and neutron-irradiated samples are summarized in Table 6. Biochemical markers confirmed the spectroscopic analysis results. Natural aging resulted in a decrease in total protein concentration and a moderate increase

 doi:10.20944/preprints202603.2309.v1

in ALT and AST levels, reflecting partial denaturation and a slowdown in metabolism.Such biochemical alterations are consistent with previous reports on radiation-induced changes in enzymatic activity and metabolic parameters in various biological systems [30–37].Further studies have extended these observations to diverse biological models, including plant systems and occupational exposure settings, confirming the nonlinear nature of biochemical responses to low-dose radiation [38–42]. In contrast, neutron irradiation enhanced enzymatic activity and increased protein and glucose levels, with the strongest effect observed at 2.16×10^{8} N/cm^2. This behavior supports the view that low-intensity irradiation promotes functional activation rather than damage, which is consistent with the observed positive shifts of the IR bands.

Table 6. Biochemical parameters of blood serum during natural aging and neutron irradiation.

Parameter	Normal range	3 days, no exposure	1.3×10^{8} N/cm^2	5 days, no impact	2.16×10^{8} N/cm^2	7 days, no exposure	3×10^{8} N/cm^2
ALT (U/L)	10:40	10.1	8.4	9.4	9.4	9.3	9.3
AST (U/L)	10:40	20	10.5	11.9	11.9	9.1	8.8
Total protein content (g/l)	64-83	68	72	74	76	69.7	74.3
Glucose (mmol/l)	3.9-5.5	6.9	7.1	7.2	8.5	6.9	7.1

As shown in Table 6, natural serum aging resulted in modest but systematic biochemical changes. ALT and AST activities increased slightly, while total protein concentration gradually decreased and glucose levels increased moderately. These trends indicate progressive dehydration, partial protein denaturation, and a gradual decline in metabolic efficiency, which are characteristic features of aging biological systems. The observed biochemical behavior correlates with negative frequency shifts in the regions of 1080-1240 cm^{-1} and 1310-1340 cm^{-1} spectra FTIR data, reflecting structural compaction and decreased mobility of protein-lipid complexes. In contrast, exposure to low thermal neutron fluxes induced a qualitatively different biochemical response. As shown in Table 6, enzymatic activity increased significantly, reaching maximum values at an intermediate fluence of 2.16×10^{8} N/cm^2, accompanied by an increase in total protein and glucose levels. This pattern indicates the activation of metabolic and enzymatic pathways rather than structural degradation. The corresponding positive shifts in the IR bands in the 1080-1240 and 2920-2960 cm^{-1} regions indicate on the weakening of hydrogen bonds and the reorganization of protein-lipid interfaces, which contributes to increased molecular mobility and enzymatic efficiency.

Notably, glucose levels in the control samples were slightly above the conventional reference range (3.9-5.5 mmol/L). This elevation is likely attributable to partial dehydration during sample storage and processing, as well as metabolic changes occurring in the serum after separation. Because all samples were handled identically, comparisons between aging and irradiation conditions remain valid. The agreement between spectroscopic and biochemical data demonstrates that low-intensity neutron irradiation induces adaptive, nonlinear biological responses rather than damage. While natural aging promotes dehydration and structural compaction, exposure to low-flux thermal neutrons triggers regulatory mechanisms associated with increased metabolic activity [43]. These results provide compelling evidence for the possibility low-flux thermal neutron hormesis at the molecular level in the biological fluids we studied.

 doi:10.20944/preprints202603.2309.v1

4. Conclusions

The conclusions presented below are based on the influence of sample preparation conditions for recording the IR spectra of the studied biocompounds, as outlined in Section 2. This study reveals various structural and functional patterns in the reactions of human blood serum and chicken egg serum under conditions of natural aging and low-flux thermal neutron irradiation. A comparative analysis shows that the observed effects are determined by both the physicochemical properties of the biological media and the applied radiation intensity. Natural aging over 3-7 days leads to a gradual compaction of the protein-lipid matrix, manifested by a negative shift in IR absorption bands in the 1080-1340 cm^{-1} range and a decrease in total protein content. These structural changes are accompanied by moderate changes in biochemical parameters, including changes in transaminase activity and glucose levels, reflecting a decrease in metabolic efficiency and a partial loss of protein structural integrity during aging. In contrast, exposure to low thermal neutron fluxes (1.3×10^8 - 3×10^8 N/cm^2) causes an opposite reaction, characterized by positive frequency shifts ($\Delta\nu = +3$ to $+8$ cm^{-1}), an increase in protein content, and an increase in enzymatic activity. These effects indicate a weakening of hydrogen bonds, a reorganization of protein-lipid complexes, and the activation of metabolic processes, indicating the development of adaptive and compensatory mechanisms rather than molecular damage. Human blood serum exhibits higher sensitivity to both aging and neutron irradiation than chicken egg serum, which exhibits greater structural stability. This difference is explained by variations in protein-lipid composition and water-binding properties, which determine the reactivity and adaptive capacity of biological systems. The results confirm the nonlinear nature of the biological response to low-intensity neutron irradiation and provide experimental results, to suggest an observation possible mechanism low-flux thermal neutron hormesis at the molecular level. Low-flux thermal neutrons do not have a destructive effect on biomolecules; instead, they promote adaptive structural reorganization and functional activation of protein-lipid systems. These data contribute to a deeper understanding of the mechanism of the effects of low thermal neutron fluxes in biological environments and can contribute to the development of biophysical models of adaptation, the assessment of radiation resistance, and further research in the field of radiation biophysics and related biomedical applications. The results illustrate a nonlinear biological response to low-intensity neutron irradiation. These observations suggest a possible hormetic-like response at the molecular level, although confirmation of radiation hormesis would require additional experiments with a broader range of neutron fluences, larger sample sizes, and inclusion of multiple donors to account for biological variability. This study was conducted using serum from a single donor, and the results should be interpreted as a demonstration of structural and biochemical responses at the molecular level rather than as population-level generalizations. Future work will include multiple donors and a broader range of neutron fluences to further validate the observed nonlinear patterns.

Acknowledgement for funding: The authors express their sincere gratitude to the Interstate Fund for Humanitarian Cooperation of the CIS Member States for the financial support of the scientific project funded by the CIS International Center for Innovation in Nanotechnology (grant No. 25-113) and the International Scientific and Technical Center (grant No. TJ -0040).

Authors' contributions: MBI: Investigation, data preparation, visualization; HH: Investigation, resources, data preparation; MMK: Formal analysis, validation; DN: Conceptualization, methodology, scientific supervision, original writing, review and editing.

Conflicts of interest: The authors declare no conflicts of interest regarding the publication of this manuscript.

Using artificial intelligence tools: Artificial intelligence tools such as ChatGPT (GPT -5.2, OpenAI) were used to improve language, grammar, format references according to APA style, and perform minor structural editing. All scientific concepts, data analysis, and interpretation of results were performed entirely by the authors. The authors reviewed and confirmed the accuracy and originality of all AI-processed text in accordance with COPE guidelines.

 doi:10.20944/preprints202603.2309.v1

References

1. Calabrese, E. J. Hormesis: From Marginalization to Mainstream: The Case for Hormesis as the Default Dose-Response Model in Risk Assessment. *Toxicol. Appl. Pharmacol.* 2004 , 197, 125-136. https://doi.org/10.1016/j.taap.2004.02.007
2. Agathocleous, E.; Calabrese, E.J. Hormesis: dose-response relationships for the 21st century: the future is now. *Curr. Opin. Toxicol.* 2019 , 13, iv-vii. https://doi.org/ 10.1016/j.tox.2019.152249
3. Luckey, T. D. *Radiation Hormesis* ; CRC Press: Boca Raton, FL, USA, 1991.
4. Yuan, Y.; Deng, L.; Zhang, C.; Liu, S.; Liu, B.; Wang, Y.; Du, G.; Zhu, J.; Zhang, S. Synergistic genotoxic effects of gamma rays and UVB radiation on human blood . *Res.* 2025 , 199, 391-404. https://doi.org/10.3390/antiox14121451
5. Makhsudov B; Nematov D; Yarov M. Combined X-ray Diffraction Analysis and Quantum Chemical Interpretation of the Effect of Thermal Neutrons on the Geometry and Electronic Properties of CdTe. *J.Mod. Nanotechnology* . 2024 , 4 , 4 . https :// doi :10.53964 / jmn.2024004 .
6. Barth, A. Infrared spectroscopy of proteins. *Biochem. Biophys. Acta* 2007 , 1767, 1073-1101. https://doi.org/10.1016/j.bbabio.2007.06.004
7. Miller, L.M.; Bourassa, M.W.; Smith, R.J. Infrared spectroscopic imaging of protein aggregates in the brain. *Biochim. Biophys. Acta* 2013 , 1828, 2339-2346. https://doi.org/10.1016/j.bbamem.2013.01.014
8. Fabian, H.; Mäntele, V. Infrared spectroscopy of proteins. In *: Handbook of Vibrational Spectroscopy* ; edited by Chalmers, J. M., Griffiths, P. R.; John Wiley & Sons: Chichester, UK, 2006.
9. Sun, T.; Wu, H.; Ji, C.; Shan, S.; Li, F. Identification of subthreshold antibiotic hormesis in global waters. *Environmental Science and Technology*. 2025 , 59 (41), 22212-22226. https://doi.org/10.1021/acs.est.5c08732 .
10. Matrobiyon, M.Kh .; Makhsudov B.I.; Khabibulloev H.; Zaidullo N. Effect of neutron irradiation on the IR spectra of human blood serum. *Int. Res. J.* 2025 , 155, 1-8. https://doi.org/10.60797/IRJ.2025.155.66
11. Manukonda, M.R.M. Chapter 3: Dose-Response Relationships. In Principles of Medical Toxicology; ThinkPlus Pharma Publications: 2025; pp. 36-59. https://doi.org/10.69613/47m4mc24 .
12. Makhsudov, B.I.; Khabibulloev, H.; Matrobiyon, M.H. Study of the impact of external factors on complex biological compounds using IR spectroscopy. *Bulletin of TNU. Series of natural sciences.* 2025 , 3, 91 - 107.
13. Makhsudov, B.I.; Khabibulloev, Kh.; Matrobillon, M.H .; Effect of neutron irradiation on the frequency shift of IR absorption bands of human blood serum. *Reports of the National Academy of Sciences of the Russian Federation* . 2025 , 68, 8, 770-777 .
14. Ekendal, D.; Vavra, J.; Khizha, M.; Haml, O.; Kotik, L.; Alaverdyan, J.; Chemusova, Z. Dosimetry of human blood criticality accidents: dicentric chromosome analysis and neutron activation as complementary methods. *Radiation Measurements* 2025 , 181, 107365. https://doi.org/10.1016/j.radmeas.2025.107365 .
15. Belskaya, L.V.; Sarf, E.A.; Solomatin, D.V. Application of IR spectroscopy for quantitative analysis of blood serum. *Diagnostics.* 2021 , 11, 2391. https://doi.org/10.3390/diagnostics11122391
16. Belskaya, L.V.; Sarf, E.A.; Solomatin, D.V. Application of IR spectroscopy for quantitative analysis of blood serum: a preliminary study. Diagnostics 2021, 11, 2391. Fedun, A.M.; Kukosh, M.V.; Gordetsov, A.S. IR spectroscopy of blood serum in the diagnosis of lung cancer. *Nizhny Novgorod Medical Journal.* 2002 , 1, 60-65. https://doi.org/10.3390/diagnostics11122391
17. Schmitt, J.; Bickess, M.; Brauer, A.; Udelhoven, T.; Lasch, P.; Naumann, D. Identification of scrapie infection in serum by IR spectroscopy. *Anal. Chem.* 2002 , 74, 3865-3868. https://doi.org/10.1021/ac015688s
18. Mokoena, D.R.; Lednev, I.K.; Sershen, S.R. Cancer detection using serum ATR-FTIR spectroscopy and multivariate data analysis. *Talanta* 2020, 214, 120857.
19. Arrondo, J. L. R.; Goni, F. M. Infrared studies of protein-lipid perturbations. *Chemical Physiology of Lipids.* 1998 , 96, 53-68. https://doi.org/10.1016/S0009-3084(98)00080-2
20. Makhsudov B; Nematov D; Yarov M. Combined X-ray Diffraction Analysis and Quantum Chemical Interpretation of the Effect of Thermal Neutrons on the Geometry and Electronic Properties of CdTe. *J.Mod. Nanotechnology.* 2024, 4, 4. https :// doi :10.53964 / jmn.2024004.
21. Domján, G.; Kaffka, K.J.; Jalsovszky, I. Rapid Analysis of Blood Serum Using Near-IR Spectroscopy. J. Near Infrared Spectrosc. 1994, 2, 67–78. https://doi.org/10.1255/jnirs.33

 doi:10.20944/preprints202603.2309.v1

22. Chen, J.; Wei, X.; Chen, P.; Xie, M.; Qian, K.; Yu, J.; Ding, W. Unveiling the Dual Nature of Molybdenum Disulfide Nanosheets: pH Modulation, Nutrient Dynamics, and Root Morphological Responses Drive Hormetic Effects in Hydroponic Tobacco Cultivation. Ind. Crops Prod. 2026, 239, 122441. https://doi.org/10.1016/j.indcrop.2025.122441
23. Jiang, M.; Lv, Z.; Chen, J.; Pan, Y.; Yu, Y.; Yu, K.; Zhang, K. Dose-Effect Analysis of 60Co-γ Radiation on Astragalus membranaceus across Life Cycle and Creation of High-Flavonoid/Super-Biomass Germplasm. J. Radiat. Res. Appl. Sci. 2026, 19, 102149. https://doi.org/10.1016/j.jrras.2025.102149
24. Pajic, J.; Milic, M.; Jurisic, V.; Vinnikov, V. Research on Low Dose Ionizing Radiation Health Effects. Front. Public Health 2025, 13, 1566179. https://doi.org/10.3389/fpubh.2025.1566179
25. Yin, J.; Ye, Y.; Gao, Y.; Xu, Q.; Su, M.; Sun, S.; Hu, S. Low-Dose Ionizing Radiation and Male Reproductive Immunity: Elucidating Subtle Modulations and Long-Term Health Implications. Int. J. Mol. Sci. 2025, 26, 2269. https://doi.org/10.3390/ijms26052269
26. Nematov, D.; Burhonzoda, A.; Khusenov, M.; Kholmurodov, K.; Doroshkevych, A.; Doroshkevych, N.; Ibrahim, M. Molecular Dynamics Simulations of the DNA Radiation Damage and Conformation Behavior on a Zirconium Dioxide Surface. Egypt. J. Chem. 2019, 62, 149–161. https://doi.org/10.21608/ejchem.2019.12981.1811
27. Nematov, D.D.; Burkhonzoda, A.S.; Khusenov, M.A.; Kholmurodov, K.T.; Doroshkevich, A.S.; Doroshkevich, N.V.; Majumder, S. Molecular Dynamics of DNA Damage and Conformational Behavior on a Zirconium-Dioxide Surface. J. Surf. Investig. 2019, 13, 1165–1184. https://doi.org/10.1134/S1027451019060430
28. Nematov, D. Molecular and Dissociative Adsorption of H2O on ZrO2/YSZ Surfaces. Int. J. Innov. Sci. Mod. Eng. 2023, 11, 21–29. http://doi.org/10.35940/ijisme.D7927.10111023
29. Alet, A.I.; Porini, S.; Riquelme, B.D.; Bisio, A.; Scifoni, E.; Galassi, M.E. Effects of Ionizing Radiations of Different Qualities and Delivery Types on Blood Cells. Biophys. Rev. 2025, 17, 1–12. https://doi.org/10.1007/s12551-025-01302-0
30. Chow, J.C.L.; Ruda, H.E. Mechanisms of Action in FLASH Radiotherapy: A Comprehensive Review of Physicochemical and Biological Processes on Cancerous and Normal Cells. Cells 2024, 13, 835. https://doi.org/10.3390/cells13100835
31. Zhang, Y.; Chen, X.; Wang, X.; Chen, J.; Du, C.; Wang, J.; Liao, W. Insights into Ionizing Radiation-Induced Bone Marrow Hematopoietic Stem Cell Injury. Stem Cell Res. Ther. 2024, 15, 222. https://doi.org/10.1186/s13287-024-03853-7
32. Holt, K.L. Biological Dosimetry and Individual Susceptibility in Chronic Low-Dose Occupational Ionizing Radiation Exposure: Implications for Worker Health Surveillance. J. Life Sci. Public Health 2026, 2, 1–8. https://doi.org/10.69739/jlsph.v2i1.1361
33. Rybacki, B.; Wysocki, W.; Zajkowski, T.; Brodzik, R.; Krawczyk, B. Effects of Microgravity, Hypergravity, and Ionizing Radiation on the Enzymatic Activity of Proteinase K. Molecules 2026, 31, 229. https://doi.org/10.3390/molecules31020229
34. Kim, E.J.; Cao, D.L.; Koh, E.H.; Kim, J.S.; Yun, S.P.; Kang, D. Alterations in Hematological, Biochemical, and Immune Parameters in Body Fluids Following Low-Dose-Rate Radiation Exposure in Mice. Int. J. Radiat. Biol. 2025, 101, 1–11. https://doi.org/10.1080/09553002.2025.2595631
35. Machado-Santelli, G.M.; Chaves, J.B. Hormesis and Cancer Therapy. In Hormesis, Brain Aging and Metabolism, 1st ed.; Rattan, S.I.S., Ed.; Academic Press: Cambridge, MA, USA, 2025; Volume 295, pp. 333–355. https://doi.org/10.1016/bs.pbr.2025.05.010
36. Seth, R.K.; Vimal, N.; Angmo, N.; Sengupta, M.; Seth, R. Low-Dose Ionizing Radiation Augmenting the Reproductive Fitness of Radio-Sterilized Moths, Spodoptera litura (Fabr.): An Approach Toward Increasing the Efficiency of 'Inherited Sterility technique' for Lepidopteran Pest Control. Int. J. Radiat. Biol. 2025, 101, 1–16. https://doi.org/10.1080/09553002.2025.2588404
37. Fahrion, J.; Gupta, S.; Mastroleo, F.; Dussap, C.G.; Leys, N. Chronic Low-Dose Rate Irradiation Induces Transient Hormesis Effect on Cyanobacterium Limnospira indica. iScience 2025, 28, 103447. https://doi.org/10.1016/j.isci.2025.111891

 doi:10.20944/preprints202603.2309.v1

38. Tokhmechi, K.; Ghorbani, A.; Koolivand, D.; Rostami, M.; Hajiloo, N. Effect of Low-Dose Gamma Irradiation on Seed-Borne Transmission of Tomato Brown Rugose Fruit Virus in Tomato. Journal of Genetic Engineering and Biotechnology 2026, 24 (1), 100644. https://doi.org/10.1016/j.jgeb.2025.100644
39. Nizomov, Z.; Asozoda, M.; Nematov, D. Characteristics of Nanoparticles in Aqueous Solutions of Acetates and Sulfates of Single and Doubly Charged Cations. Arab. J. Sci. Eng. 2022, 47, 867–873. https://doi.org/10.1007/s13369-021-06273-4
40. Doroshkevich, A.S.; Nabiev, A.A.; Shylo, A.V.; Pawlukojć, A.; Doroshkevich, V.S.; Glazunova, V.A.; Zelenyak, T.Y.; Doroshkevich, N.V.; Rahmonov, K.R.; Khamzin, E.K.; Burhonzoda, A.S.; Khusenov, M.A.; Kholmurodov, K.T.; Majumder, S.; Balasoiu, M.; Madadzada, A.; Bodnarchuk, V.I. Frequency Modulation of the Raman Spectrum at the Interface DNA–ZrO2 Nanoparticles. Egypt. J. Chem. 2019, 62, 13–20. https://doi.org/10.21608/ejchem.2019.16447.1994
41. Nematov, D.; Kholmurodov, K.; Stanchik, A.; Fayzullaev, K.; Gnatovskaya, V.; Kudzoev, T. On the Optical Properties of the $Cu_2ZnSn[S_{1-x}Se_x]_4$ System in the IR Range. Trends Sci. 2023, 20, 4058. https://doi.org/10.48048/tis.2023.4058
42. Ryan, T.L.; Escalona, M.B.; O'Brien, K.; Tan, Y.; Kanagaraj, K.; Taveras, M.; Nemzow, L.; Phillippi, M.; Deoli, N.; Wang, E.; Shuryak, I.; Garty, G.; Turner, H.C.; Balajee, A.S. Biological Effects of Conventional and Ultra High Dose Rate Radiation in Human Cells. Scientific Reports 2026, 16, 100. https://doi.org/10.1038/s41598-025-33817-7
43. Kim, J.H. Radiation Hormesis and Reactive Oxygen Species-Mediated Stress Priming in Plants. Plant Science 2025, 356, 112602. https://doi.org/10.1016/j.plantsci.2025.112602